Polymer 50 (2009) 366–374

Contents lists available at ScienceDirect

Polymer

journal homepage: www.elsevier.com/locate/polymer

Silk–elastinlike protein polymer hydrogels: Influence of monomer sequence on physicochemical properties

Ramesh Dandu [a,2], Arthur Von Cresce [a,1,2], Robert Briber [b], Paul Dowell [a], Joseph Cappello [c], Hamidreza Ghandehari [a,d,*]

[a] Center for Nanomedicine and Cellular Delivery and Department of Pharmaceutical Sciences, University of Maryland, Baltimore, MD, USA
[b] Department of Materials Science and Engineering, University of Maryland, College Park, MD, USA
[c] Protein Polymer Technologies, Inc., San Diego, CA, USA
[d] Department of Pharmaceutics and Pharmaceutical Chemistry and Bioengineering, Center for Nanomedicine, Nano Institute of Utah, University of Utah, Salt Lake City, UT, USA

ARTICLE INFO

Article history:
Received 3 September 2008
Received in revised form
18 November 2008
Accepted 18 November 2008
Available online 3 December 2008

Keywords:
Genetically engineered polymers
Silk–elastinlike protein polymers
Hydrogels

ABSTRACT

Silk–elastinlike protein polymer, SELP-815K, with *eight* silk and *fifteen* elastin units and a lysine (K) modified elastin, was genetically engineered with longer silk and elastin units compared to existing hydrogel forming analogs (SELP-415K and SELP-47K). Hydrogels of the three SELPs (with similar MWs) were investigated for their structure–function relationships. Results indicate that equilibrium swelling ratio in these hydrogels is a function of polymer structure, concentration, cure time and ionic strength of media. Swelling was not influenced by the changes in pH. Storage moduli observed by dynamic mechanical analysis and the Debye–Bueche correlation length obtained from small-angle neutron scattering provided structural insight that suggests the cross-linking densities in these hydrogels follow the order SELP-47K > SELP-815K > SELP-415K. These results allude to the importance of the length of elastin blocks in governing the spacing of the cross-linked hydrogel network and that of silk in governing the stiffness of their 3-dimensional structures.

1. Introduction

The majority of polymeric matrices used for biomedical applications are either naturally occurring or chemically synthesized. Natural polymers are generally biocompatible and have proven efficacies in certain applications including drug delivery and tissue engineering. However, they are not amenable to structural modifications of their architecture for specific needs. Chemical synthesis, on the other hand allows for customization of polymer structure. Chemical synthesis, however, often results in random copolymers with unspecified monomer sequences and statistical distribution of molecular weights. This limits the ability to correlate polymer structure with function and has prompted the need for exploration of novel synthetic strategies that allow exquisite control over monomer sequence and polymer length [1].

Advances in recombinant DNA technology have inspired the development of genetically engineered protein polymers that offer the advantages of biocompatibility of natural polymers on one hand and control over polymer architecture on the other hand [2–4]. These polymers are stereoregular, monodisperse and can be precisely engineered to have desired structure(s), sequence(s) and thereby envisioned functionalities [4,5]. Their unique structural features have been explored extensively and applied in the fields of drug and gene delivery and tissue engineering [6,7]. One unique

Abbreviations: A (Ala), Alanine (amino acid); ANOVA, Analysis of variance; bp, Base pairs; C (Cys), Cysteine (amino acid); CGC, Critical gel concentration; D (Asp), Aspartic acid; Da, Daltons; DNA, Deoxyribonucleic acid; E (Glu), Glutamic acid; *E. coli* HB101, *Escherichia coli* strain HB101; F (Phe), Phenylalanine; G (Gly), Glycine (amino acid); G^*, Complex shear modulus; GAGAGS, Silk-like repeat; GVGVP, Elastinlike repeat; H (His), Histidine; I (Ile), Isoleucine; K (Lys), Lysine; L (Leu), Leucine; M (Met), Methionine; MALDI-TOF-MS, Matrix-assisted laser desorption ionisation time-of-flight mass spectroscopy; MW, Molecular weight; N (Asn), Asparagine; P (Pro), Proline; Q (Gln), Glutamine; Q, Weight equilibrium swelling ratios of hydrogels (q); R (Arg), Arginine; S (Ser), Serine; S:E, Silk to elastin ratio; SAP, Shrimp alkaline phosphatase; SDS-PAGE, Sodium dodecyl sulfate polyacrylamide gel electrophoresis; SELP, Silk–elastinlike polymers; T, Thymine (deoxyribonucleic acid base); T (Thr), Threonine (amino acid); V (Val), Valine; W (Trp), Tryptophan; W_d, Dry hydrogel weight; W_s, Weight of swollen hydrogels; Y (Tyr), Tyrosine.

* Corresponding author. Department of Pharmaceutics and Pharmaceutical Chemistry and Bioengineering, Center for Nanomedicine, Nano Institute of Utah, University of Utah, 383 Colorow Road, Room 343 Salt Lake City, UT 84108, USA. Tel.: +1 801 587 1566; fax: +1 801 585 0575.
E-mail address: hamid.ghandehari@pharm.utah.edu (H. Ghandehari).
[1] Present address: Fischell Department of Bioengineering, University of Maryland, College Park, MD, USA.
[2] These authors contributed equally to this work.

0032-3861/$ – see front matter © 2008 Elsevier Ltd. All rights reserved.
doi:10.1016/j.polymer.2008.11.047

class of genetically engineered biomaterials is the family of silk–elastinlike protein polymers (SELPs) [2]. SELPs are block copolymers composed of alternately repeated silk (GAGAGS) and elastinlike (GVGVP) units. Elastin units confer aqueous solubility and silk units provide crystallinity and mechanical strength for these polymers. By carefully controlling the sequence and length of the silk and elastin repeats it is possible to produce a variety of SELPs with diverse structural and material properties [8]. Two polymer analogs, SELP-47K and SELP-415K (Scheme 1A and B), with four silk and seven and fifteen elastin units respectively and an additional elastin with lysine (K) modification in each, are capable of self-assembly and irreversible sol-to-gel transition at 37 °C [9,10]. This allows their convenient mixing with biologicals such as naked DNA and viral vectors at room temperature minutes prior to injection in the body [11,12]. These analogs have been used for localized gene delivery [13], and tissue engineering [14]. Our previous observations indicate that increase in the length of elastin units in SELP-415K (compared to SELP-47K) resulted in hydrogels with larger swelling ratio and increased release of bioactive agents in vitro [10,13]. However the low silk to elastin ratio (S:E) in SELP-415K resulted in gel formation in a narrower polymer concentration (10–12 wt%) compared to that of SELP-47K (4–12 wt%) limiting the compositions available for biomedical applications including localized delivery needs. Design of a new hydrogel forming polymer with the same S:E ratio as SELP-47K but with longer elastin units than SELP-415K, namely SELP-815K (Scheme 1C), could facilitate enhanced bioactive agent release from the hydrogels while the longer silk block could maintain robust cross-linking.

Here we report on the biosynthesis of SELP-815K (Scheme 1C) with eight silk and fifteen elastin units and an extra elastin unit with a lysine (K) replacement in the monomer repeats. SELP-815K polymer with 6 repeats (SELP-815K-6mer) was selected to have similar molecular weight as that of SELP-415K-8mer and SELP-47K-13mer to allow a comparison of SELP analogs while maintaining the length of polymer chains approximately constant. Using an array of characterization tools we examined the influence of these structural changes on equilibrium swelling under various environmental conditions, mechanical properties and pore structure of the hydrogels.

2. Experimental section

2.1. Materials

Restriction endonuclease enzymes BanI, BanII, BamHI and EcoRV, and T4 DNA Ligase were purchased from New England Biolab (Beverly, MA). DNA ladder and Shrimp alkaline phosphatase (SAP) were purchased from Fermentas (Hanover, MD). QIAprep Spin Miniprep kits, QIAGEN Plasmid Maxi kits and QiaQuick Gel Extraction kits were obtained from Qiagen (Valencia, CA). Pro-Bond™ purification system was obtained from Invitrogen (Carlsbad, CA). *Escherichia coli* HB101 competent cells were purchased from Promega (Madison, WI). Bio-Spin®30 Tris columns, Precast Tris–HCl 4–15% linear gradient gels, Tris–glycine SDS buffer, Precision Plus Protein™ standards Bio-Safe™ Coomassie stain were obtained from Bio-Rad (Hercules, CA). pHydrion buffer capsules were obtained from Micro-Essential Laboratory (Brooklyn, NY).

A MDPVVLQRRDWENPGVTQLNRLAAHPPFASDPMG AGSGAGAGS [(GVGVP)$_4$ GKGVP (GVGVP)$_3$ (GAGAGS)$_4$]$_{12}$ (GVGVP)$_4$ GKGVP (GVGVP)$_3$ (GAGAGS)$_2$ GAGA MDPGRYQDLRSHHHHHH

B MDPVVLQRRDWENPGVTQLNRLAAHPPFASDPMG AGSGAGAGS [(GVGVP)$_4$ GKGVP (GVGVP)$_{11}$ (GAGAGS)$_4$]$_7$ (GVGVP)$_4$ GKGVP (GVGVP)$_{11}$ (GAGAGS)$_2$ GAGA MDPGRYQDLRSHHHHHH

C MDPVVLQRRDWENPGVTQLNRLAAHPPFASDPM [GAGS (GAGAGS)$_2$ (GVGVP)$_4$ GKGVP (GVGVP)$_{11}$ (GAGAGS)$_5$ GAGA]$_n$ MDPGRYQDLRSHHHHHH

Scheme 1. The amino acid sequence of SELPs. A. SELP-47K-13mer (MW – 69,814 Da). B. SELP-415K-8mer (MW – 71,500 Da). C. SELP-815K where $n = 3$, 4, 5, and 6 with MW – 35,638, 45,549, 55,461, 65,374 Da respectively. The properties of SELP-815K-6mer were compared to SELP-47K and SELP-415K. All polymers are composed of head and tail portions, and a series of silk-like (GAGAGS) and elastin-like (GVGVP) repeats (primary repetitive sequence in bold, number of repeats highlighted in gray). For amino acids see abbreviations.

2.2. Biosynthesis of SELP-815K

The cloning and expression vectors, pPT340, pSY1378 and pPT317 (Protein Polymer Technology, Inc., San Diego, CA) were propagated in *E. coli* HB101 and purified using a Qiagen Giga Kit according to the manufacturer's instructions. The concentration and purity of the plasmids were obtained using Ultrospec 4000 (Amersham Biosciences, Piscataway, NJ) at 260 and 280 nm. Plasmids with A_{260}/A_{280} ratio in the range of 1.8–2.0 were used. Plasmids were electrophoresed on a 0.9% agarose gel and stained with ethidium bromide to verify the absence of genomic DNA and the integrity of the plasmid. The general biosynthetic methodology is outlined in Scheme 2. The details of the methodology are described below.

2.3. Synthesis of the monomer gene segment. I

Plasmid pPT340 (containing SELP-415K monomer gene) was restriction digested with BanII to produce an SELP-215K oligonucleotide (184 bp), which was separated and purified from the reaction mixture by agarose gel electrophoresis followed by gel extraction using Qiagen's gel extraction kit (Qiagen). II. Plasmid pSY1378 (containing 6 silk units) was restriction digested with BanII for 1 h at 37 °C to linearize the plasmid. Enzyme was removed from the reaction using Micropure-EZ (Millipore) columns and the linearized plasmid was treated with shrimp alkaline phosphatase (NEB Labs) for 2 h at 37 °C. SAP was removed by agarose gel electrophoresis, and DNA was purified by gel extraction using Qiagen's gel extraction kit (Qiagen). III. The acceptor plasmid pSY1378 (from II) and the SELP-215K insert (from A) were ligated at a 1:1 molar ratio in the presence of T4 ligase for 16 h at 16 °C. The ligation mixture was used to transform chemical competent cells (Max efficiency Dh5α, Invitrogen) and plated on agar plate containing chloramphenicol. Colonies were picked, propagated and plasmid DNA was purified using Qiagen's miniprep (Qiagen). The presence of SELP-815K monomer in the purified pSY1378 clone was validated by restriction digestion, on either side of the cloning site (BanII), with BanI, followed by agarose gel electrophoresis to visualize a 384 bp fragment (SELP-815K) using ethidium bromide staining (Fig. 1A). The structure of the SELP-815K monomer gene segment was confirmed by fluorescence based automated DNA sequencing using appropriate sequencing primers (Fig. 1B).

2.4. Synthesis of the polymer gene segment. IV

A DNA fragment encoding the SELP-815K monomer was excised from a parental plasmid as a BanI fragment. SELP-815K monomers self-ligated in the presence of T4 DNA ligase to form 815K multimers followed by agarose gel electrophoresis and visualization using ethiduim bromide (Fig. 1C). V. Expression vector pPT317 was restriction digested with BanI for 1 h at 37 °C, enzyme was removed using Micropure-EZ columns and treated with shrimp alkaline phosphatase (NEB Labs) for 2 h at 37 °C, and DNA was purified by agarose gel electrophoresis followed by gel extraction. DNA

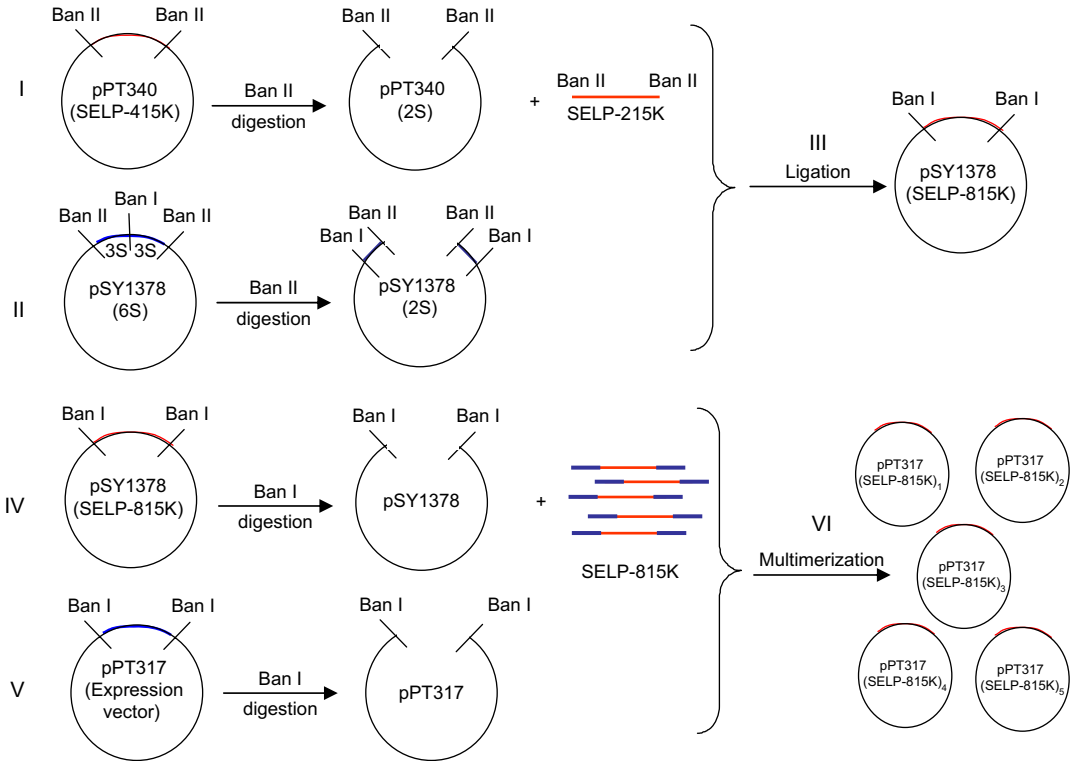

Scheme 2. Biosynthetic strategy for SELP-815K analogs.

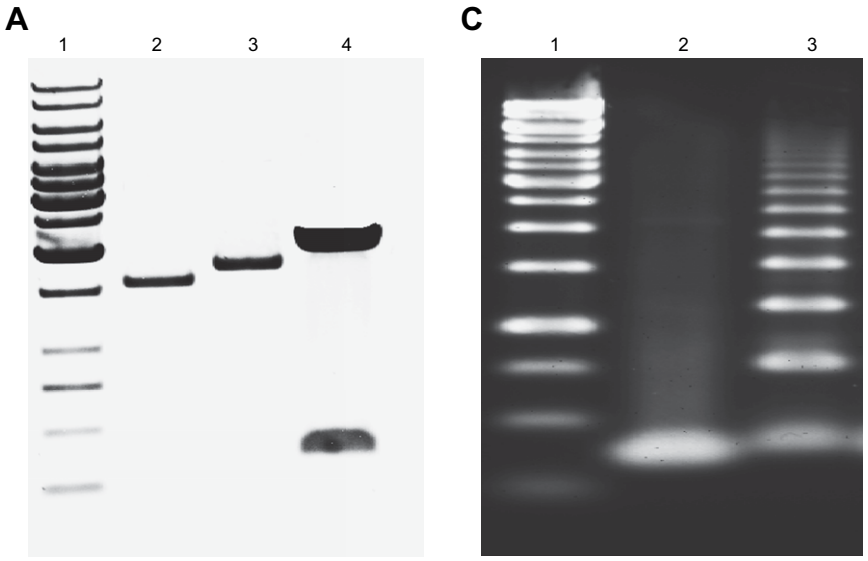

B

GGCACCCGCTCCGCTTCCTGCTCCAGCACCTGAGCCAGCGCCTGCG
CCGGATCCTGCGCCCGCGCCA**GAGCCC**GCGCCTGCGCCGCTACCA
GCACCCGCTCCCGGGACGCCAACTCCAGGAACTCCTACACCCGGC
ACTCCTACTCCCGGTACGCCTACTCCTGGTACGCCAACTCCAGGAA
CTCCTACACCCGGCACTCCTACTCCCGGTACGCCTACTCCTGGTAC
GCCTACACCTGGTACTCCAACGCCCGGCACACCTACCCCCGGAACA
CCTTTTCCAGGTACACCAACTCCCGGAACGCCTACACCCGGAACAC
CGACACCTGGCACTCCAACACCA**GAGCCC**GCGCCAGCTCCAGAAC
CGGCTCCTGCACCGCTGCC**GGCACC**

Fig. 1. Analytical gel electrophoresis of SLEP-815K monomer. A. Lane 1 GeneRuler™ 1 kb DNA ladder (0.25–10 kDa); lane 2: linearized pSY1378 with SLP-6; lane 3: linearized pSY1378 after SELP-215K insertion; lane 4: BanI digest of pSY1378 after SELP-215K insertion (linearized plasmid and SELP-815K monomer). B. Lane 1 GeneRuler™ 1 kb DNA ladder (0.25–10 kDa); lane 2: SELP-815K monomer insert; lane 3: self-ligated SELP-815K monomer mixture (1-mer, 2-mer, 3-mer, 4-mer, upto *n*-mer). C. DNA sequencing data for SELP-815K monomer gene segment constructed from insertion of SELP-215K (underlined) inside SLP-6 sequence resulting in a 384 bp segment flanked by BanI restriction endonuclease recognition sites (highlighted in gray).

integrity was checked by running the SELP-815K insert and the open, SAP treated pPT317 on agarose gel electrophoresis. VI. The expression vector pPT317 (SAP treated) and the SELP-815K insert were allowed to undergo random multimerization in the presence of T4 DNA ligase for 16 h at 16 °C. The ligation mixture was used to transform chemical competent cells (Max efficiency Dh5α, Invitrogen, Carlsbad, CA) and plated on agar plate containing Kanamycin. The desired 6-mer was isolated through a combination of colony PCR screening and restriction digestion procedures. A series of vectors were obtained containing 1-, 2-, 3-, 4-, 5- and 6-mer inserts of the BanI monomer.

2.5. Small scale expression and purification

6 mL overnight cultures were grown in the presence of 10 μg/mL kanamycin at 30 °C. The overnight cultures were diluted into 54 mL of LB containing 10 μg/mL kanamycin and grown for 3 h at 30 °C. The temperature was increased to 42 °C to induce expression and the cultures were grown for an additional 2 h at the permissive temperature. The culture was centrifuged to pellet the cells and the resulting cell pellet was lysed in 1 mL of the commercially available BugBuster® protein extraction reagent (Novagen) containing protease inhibitors. Insoluble material was separated from soluble clarified lysates by centrifugation and recombinant SELPs were purified using Ni-NTA spin columns (Qiagen). Purified recombinant SELPs were eluted in buffer containing 50 mM NaH_2PO_4/300 mM NaCl/250 mM imidazole/pH 8.0.

2.6. Molecular characterization of SELP-815K polymers

The integrity of the constructs was verified by SDS-PAGE and MALDI-TOF analysis. The primary amino acid structure of these polymers is outlined in Scheme 1C. Eluted samples were diluted with water before MALDI-TOF analysis. Amino acid content analysis of SELP-815K-6mer was carried out by Commonwealth Biotechnologies, Inc. (Richmond, VA) by chromatographic measurement of derivatized peaks after hydrolysis of the sample in 6 N HCl at 110 °C for 20 h (Table 1).

2.7. Preparation of hydrogels

Frozen polymer stock solutions (12 wt%) of SELP-47K, 415K and 815K were thawed for 5 min in a room-temperature water bath. Seven polymer compositions, three each (4 wt%, 8 wt% and 12 wt%) of SELP-47K and -815K and one (12 wt%) of SELP-415K, were obtained by dilution using dPBS. They were gently mixed to produce homogenous solutions that were transferred to a disposable syringe (1 mL), covered with parafilm and incubated at 37 °C to induce hydrogel formation. Hydrogels were cured (4–48 h) and cut into 50 mm^3 cylindrical discs using a razor blade. Hydrogel discs were placed in 1 mL of 1× dPBS and incubated at 37 °C, 120 rpm in a shaking incubator. At predetermined time points hydrogels were retrieved and analyzed for their swelling ratio.

Table 1
Amino acid composition analysis of the SELP-815K polymers.

Amino acids	SELP-815K-6mer	
	Res/Mol Th[a]	Res/Mol Ob[a,b]
Gly	344	333.30
Val	189	192.48
Ala	105	101.66
Pro	102	118.58
Ser	50	45.59
As(x)	7	7.37
His	7	5.45
Arg	5	3.93
Gl(x)	4	4.54
Leu	4	3.62
met	3	1.70
Lys	6	5.31
Thr	1	1.25
Tyr	1	1.12
Trp	1	0.00
Phe	1	1.52

[a] Res/Mol Th, theoretical number of residues per mole; Res/Mol Ob, observed number of residues per mole.
[b] Based on observed molecular weight.

2.8. Equilibrium swelling studies

SELP compositions capable of forming physically robust hydrogels were evaluated for degree of swelling as described previously [15]. Briefly, the soluble polymer fraction in the hydrogels was removed by washing the hydrogels for a week in 1× dPBS under mild agitation at 37 °C. The weight equilibrium swelling ratio (q) was experimentally determined using Eq. (1) [13,15].

$$q = \frac{W_s}{W_d} \tag{1}$$

where, W_s is the swollen hydrogel weight and W_d is the dry hydrogel weight. Swollen hydrogels were removed from test conditions, gently blotted with a lint-free wipe and weighed. Dry hydrogels were obtained by placing swollen hydrogels in a dessicator containing Drierite for 5 days. Gel discs were then weighed and placed into a vacuum oven at 30 °C for 24 h and then re-weighed. No change in dry hydrogel weight was found following vacuum drying.

Influence of cure time (448 h) and environmental conditions such as ionic strength of the media (0.016–1.6 M), pH (2–12) and temperature (4–47 °C) on the weight equilibrium swelling ratio of these hydrogels was determined. Triplicate samples were analyzed and statistical differences were determined using ANOVA and student t-test at $\alpha = 0.05$.

2.9. Dynamic mechanical analysis (DMA)

Dynamic mechanical analysis was performed at the Functional Macromolecular Laboratory of the University of Maryland, College Park on a TA Instruments Q800 DMA using a submersion compression clamp. The DMA was operated in controlled strain mode with an oscillation frequency of 1 Hz. All experiments were performed on cylindrical SELP hydrogels with a diameter of 12.5 mm and thickness of 2.5 mm prepared by incubating at 37 °C for 4 h using the method described above. Tests were carried out at room temperature and with ~4 mL of buffer solution surrounding the sample to maintain hydration. Single frequency multi-strain analysis (strain sweep) was carried out on samples in the 0.2–2.0% strain range. Data was collected and analyzed up to 2% strain or until the samples failed (fractured) at higher strain amplitudes.

2.10. Small-angle neutron scattering (SANS)

SELP hydrogels used for SANS were prepared as described above. Water molecules in the hydrogel samples were exchanged with D_2O for 24 h prior to sample analysis to provide neutron scattering contrast. Titanium sample cells with quartz windows were used to contain all SELP samples and had a fixed 1 mm sample length. Liquid SELP samples for sol-to-gel transition (kinetic) analysis were diluted with D_2O to 4 wt% and 8 wt% for the experiment, and the resulting D_2O/H_2O background was factored into the data processing algorithm for those samples. SANS was performed using the NG-7 30 m beamline of the Center for Neutron Research

(NCNR) at the National Institute for Standards and Technology (NIST) in Gaithersburg, MD [16]. The neutrons of wavelength 6 ± 0.110 Å were used for scattering. Solid SELP sample data was collected at a detector distance of 1 m and 10 m to provide a combined q-range of $0.004\ \text{Å}^{-1} < Q < 0.4\ \text{Å}^{-1}$. Kinetic samples were collected only at a detector distance of 7.75 m due to the time constraints of the kinetic experiment, giving a q-range of $0.005\ \text{Å}^{-1} < Q < 0.08\ \text{Å}^{-1}$. Kinetic SELP samples were injected into the cell as liquids and then maintained at 37 °C in the neutron beam using a temperature-controlled sample changer.

Data collected from SANS was processed using standard NIST-developed routines for IGOR (Wavemetrics, Lake Oswego, OR) which perform corrections for instrument and environmental backgrounds as well as solvent baseline scattering. SANS data was analyzed using the IRENA modeling package developed by Dr. Jan Ilavsky of Argonne National Laboratory, Chicago, IL [17].

3. Results and discussion

3.1. Molecular characterization of SELP-815K

SELP-815K oligomers 3- ,4- ,5- and 6-mers were identified by MALDI-TOF (Fig. 2). The theoretical/observed$_{\text{MALDI-TOF}}$ masses are as follows: SELP-815K-3mer [35,637.81/35,550.08]; SELP-815K-4mer [45,549.88/45,155.76]; SELP-815K-5mer [55,461.96/54,904.24]; SELP-815K-6mer [65,374.03/64,865.53]. SELP-815K-6mer has molecular weight (65,374 Da) that is similar to that of SELP-47K-13mer (69,814 Da) and SELP-415K-8mer (71,500 Da). Amino acid content analysis of SELP-815K-6mer is described in Table 1. This allows the correlation of polymer structure with characteristics while maintaining the molecular weights approximately constant, since it is known that variations in molecular weight of polymers in three-dimensional polymeric networks influence network characteristics [18]. Henceforth, SELP-47K-13mer, SELP-415K-8mer and SELP-815K-6mer will be addressed as SELP-47K, SELP-415K and SELP-815K respectively (Scheme 1A–C).

3.2. Critical gelation concentration (CGC)

CGC is the concentration above which the cross-links resulting in the hydrogels are physically robust to form a non-flowing gel phase. This is generally a function of the structure, molecular weight and concentration of the polymer. However since the SELP hydrogel analogs under study have similar molecular weights the differences in their gelation properties are a function of their composition (concentration and structure). It was observed that when cured for 4 h SELP-815K formed hydrogels in the concentration range 4–12 wt% similar to SELP-47K, whereas in the case of SELP-415K a minimum of 12 wt% concentration was necessary for gel formation. This can be attributed to similar silk to elastin ratio (S:E) in case of SELP-47K and -815K allowing the formation of comparable number of silk cross-links per fibril. The lower S:E ratio in the case of SELP-415K presents lesser number of hydrogen bonding (silk) sites for formation as compared to the higher silk containing analogs (-47K and -815K) thereby requiring more polymer chains (or higher CGC) to self-assemble and form robust hydrogels [10].

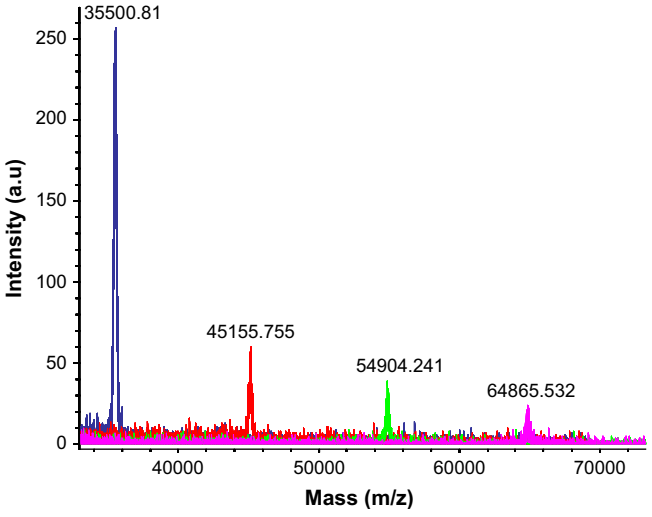

Fig. 2. Matrix-assisted laser desorption ionisation time-of-flight (MALDI-TOF) spectra. SELP-815K-3mer – 3550.081 Da, SELP-815K-4mer – 45,155.755 Da, SELP-815K-5mer – 54,904.241 Da, SELP-815K-6mer – 64,865.532 Da.

3.3. Influence of polymer structure, concentration and cure time on swelling

The degree of swelling (q) in SELPs is predictive of their pore sizes and thereby their release and mechanical properties. Swelling in SELPs is predominantly a function of polymer structure, concentration and cure time [10,13,15]. Increase in polymer concentration resulted in a lower q observed for SELP-47K and -815K compositions (Fig. 3, Panels B and D). Presence of larger number of SELP fibrils per unit volume at higher polymer concentrations allows formation of more points of contact for hydrogen bonding between the silk units contributing to a tighter network and a correspondingly lower swelling ratio.

At similar polymer concentration (12 wt%) swelling ratio of SELPs at 4 h cure time and 0.016 and 0.16 molar ionic strength is in the order SELP-415K > SELP-815K > SELP-47K (Fig. 3, Panels C and D). The lower S:E ratio and the increased length of the elastin blocks in case of SELP-415K allow lesser hydrogen bonding capability resulting in a much higher swelling ratio compared to SELP-47K and SELP-815K. SELP-47K and -815K have similar S:E ratio(s), however, the presence of longer elastin blocks in case of SELP-815K allows larger spacing of the silk cross-links resulting in a higher swelling ratio ($p < 0.05$).

Increase in cure time (4 h, 24 h and 48 h) resulted in a decrease in observed q (Fig. 4A). Prolonged cure time permits longer time for the silk units to align and configure three dimensionally to form more and/or stronger cross-links resulting in a tighter network and a correspondingly smaller q. As a consequence at higher cure times the difference in swelling ratio of the hydrogels is diminished.

3.4. Influence of temperature, ionic strength and pH on swelling

The self-assembly and the three-dimensional structure of the SELPs are driven by the competition of the hydrophobic elastin with the polar residues for the same water molecule(s) for hydration [19]. The influence of ionic strength of the media at constant pH was examined in the 0.016–1.6 M range. Increase in the ionic strength of the media for the 12 wt% hydrogels caused a decrease in swelling ratio ($p < 0.05$) (Fig. 3C). These differences are more pronounced in 0.16–1.6 M range compared to 0.016–0.16 M. At higher ionic strength (1.6 M) hydrogel swelling decreased (compared to 0.016 M) as much as 44%, 52% and 47% respectively for the three analogs -47K, -415K and -815K. This decrease in swelling is not significant at lower polymer concentrations (4 wt% and 8 wt%) for SELP-47K and -815K in the ionic strength range of 0.016–0.16 M (Fig. 3D). However, significant decrease in swelling occurred when the ionic strength increased from 0.16 to 1.6 M ($p < 0.001$). This can be explained by the counter-ion shielding of polar residues with increased ionic strength resulting in the attainment of equilibrium swelling with much lesser water uptake

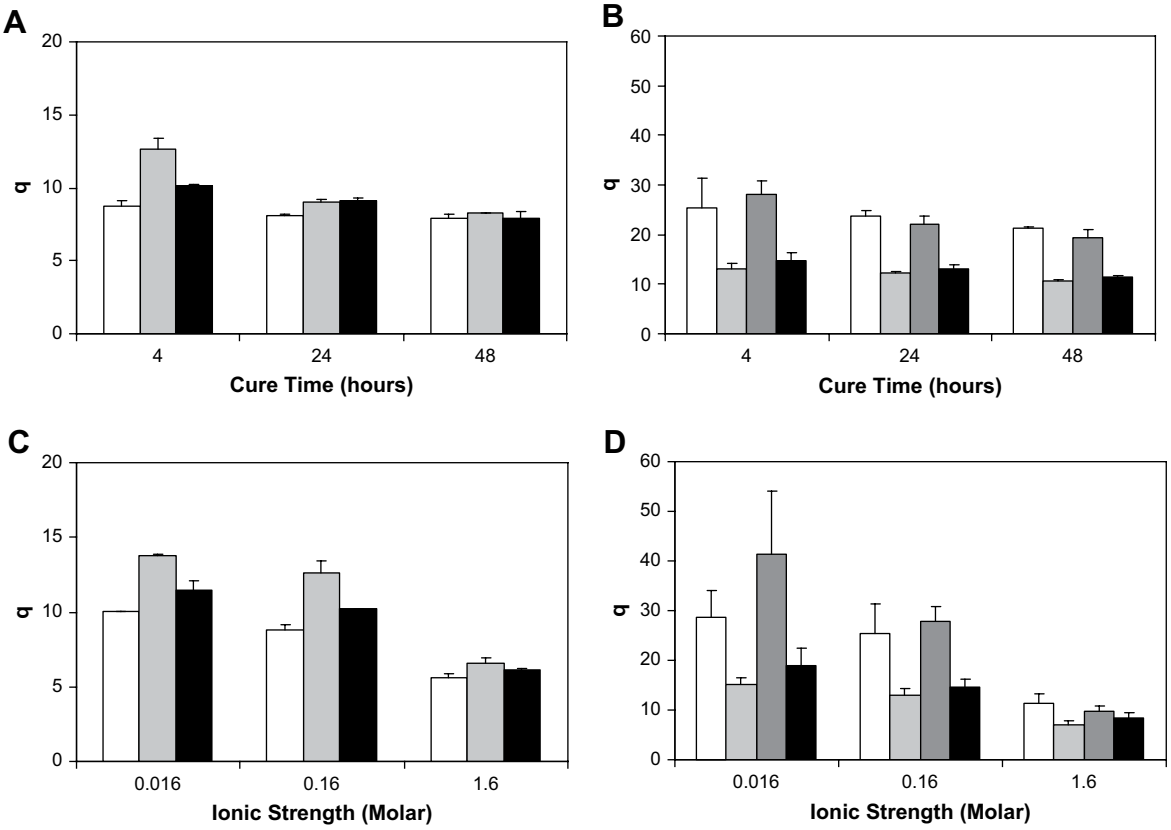

Fig. 3. Effect of gelation (cure) time and ionic strength of the media (pH 7.4) on the weight equilibrium swelling ratio (q) as a function of polymer composition. Panels A and C. White – SELP-47K (12 wt%), Gray – SELP-415K (12 wt%), Black – SELP-815K (12 wt%). Panels B and D. White – SELP-47K (4 wt%), Light gray – SELP-47K (8 wt%), Dark gray – SELP-815K (4 wt%), Black – SELP-815K (8 wt%). Bars represent mean value ± one standard deviation ($n = 3$).

and a correspondingly lower q. Moreover the influence of a higher osmotic gradient appears to increase water outflow from the hydrogels resulting in a lower equilibrium swelling at high molar concentrations.

Increase in temperature from 4 °C to 47 °C does not alter the swelling ratio of SELP-47K and -815K (Fig. 4A). However, in case of SELP-415K as previously observed [10] there is a decrease in q with increase in temperature ($p < 0.05$). This can be explained by the inverse temperature solubility transition observed in elastin-like units in SELP and elastin-like polymers (ELP) [10,20]. The stability of q in the cases of SELPs with higher S:E ratio (SELP-47K and -815K) can be explained by the formation of a rigid cross-linked structure due to the presence of an increased number of silk units. The temperature sensitivity observed in the case of SELP-415K is possibly due to the formation of less rigid, physical cross-links as a result of the increase in the length of the elastin blocks that separate the shorter silk-like cross-links.

The swelling ratios of all the compositions of SELPs were a function of polymer structure and concentration in the pH range of 2–12 and were not influenced by changes in pH (Fig. 4B). This is supported by previously observed results for SELP-47K and -415K, which comply with hydrophobicity induced pK_a shifts in elastin

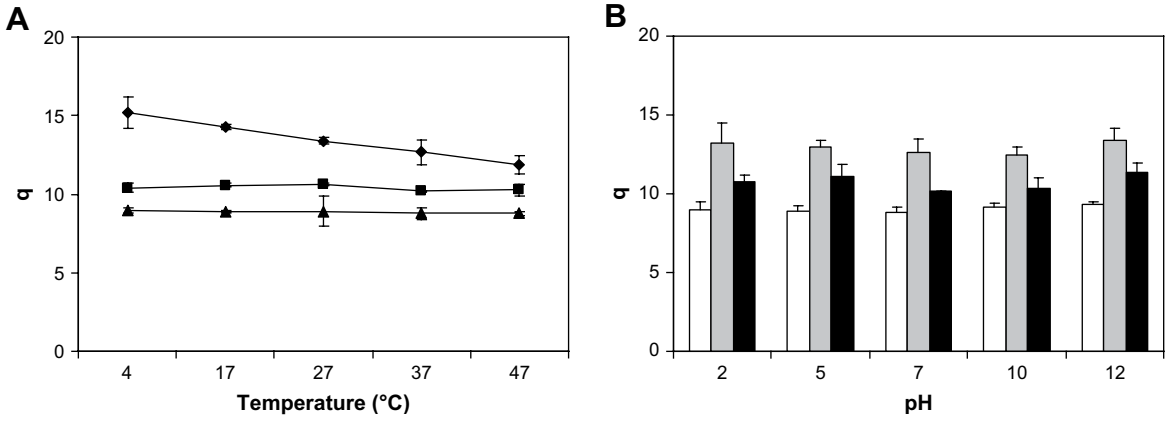

Fig. 4. Influence of environmental conditions on q as a function of polymer structure for 12 wt% SELP hydrogels cured for 24 h at 37 °C. A. Effect of temperature on q in PBS (pH 7.4, $\mu = 0.16$), symbols represent SELP-47K (▲), SELP-415K(◆) and SELP-815K (■). B. Effect of pH on q at 37 °C ($\mu = 0.16$). White – SELP-47K, Gray – SELP-415K, Black – SELP-815K (12 wt%). Symbols and bars represent mean value ± one standard deviation ($n = 3$).

based protein polymers [21]. The presence of the head and tail amino acid residues affecting the net pK_a and the nature and the extent of physical cross-linking between the silk units may also contribute to the stability of the network in the pH range tested.

3.5. Dynamic mechanical analysis (DMA)

Polymer composition and cure time are the governing factors that control the cross-linking density of SELP hydrogels. Mechanical properties are largely governed by cross-linking density. Previously reported frequency ramp tests at constant strain for SELP hydrogels indicate that the structure and concentration of the polymers determine the mechanical properties of these constructs and that increase in the frequency of applied strain does not alter the mechanical behavior of SELP-47K and -415K hydrogels [22]. The current study investigates the mechanical properties of SELP hydrogels at constant temperature and pH as a function of compressive strain. The initial analysis of the samples was restricted to hydrogels cured for 4 h at 37 °C to allow comparison with previous swelling and release data [13]. The storage modulus (stiffness) of SELP hydrogels was analyzed as a function of compression using DMA.

Initial analysis revealed that the SELPs respond in a linear fashion to stress up to 1.5% strain, at which point they rapidly strain-harden and fail between 1.7% and 1.8%. SELP-415K was an exception, as it remained intact throughout a greater strain range (up to 2.0%, data not shown). Thus, the SELPs were compared through data taken from strains up to 1.5%. As expected with increasing strain, there was an increase in the observed storage moduli of the SELP hydrogels in the order SELP-47K > SELP-815K > SELP-415K ($p < 0.05$) (Fig. 5). The storage moduli at 1.5% strain for SELP-47K, -415K and -815K are 5.09 MPa, 1.98 MPa, and 0.52 MPa respectively. These observations are consistent with the observed swelling ratios and the structure of the SELP analogs under study indicating that the distance between the physical cross-links spaced by elastin units, and the length of the silk-like units are key determinants of the mechanical behavior of these hydrogels.

The storage moduli of SELP hydrogels are non-linear with intermittent "step jump" of the modulus at different strains. SELP-47K produced two spikes first at 0.9% and 1.37% strain before the gels failed (fractured) at higher strains. SELP-47K hydrogels, owing to the higher frequency of crystalline silk cross-links than both SELP-815K and -415K, exhibited the highest storage modulus of the three SELPs. The presence of longer elastin blocks separating the silk blocks in SELP-815K and -415K renders these hydrogels much more flexible and less resistant to the changes in physical conformation. A combination of factors such as the separation of the silk units by longer elastin repeats in SELP-415K and SELP-815K compared to SELP-47K and their influence on the rate and extent of formation of the necessary silk cross-links that stabilize the 3-dimensional network may explain the observed storage moduli patterns observed for these hydrogels.

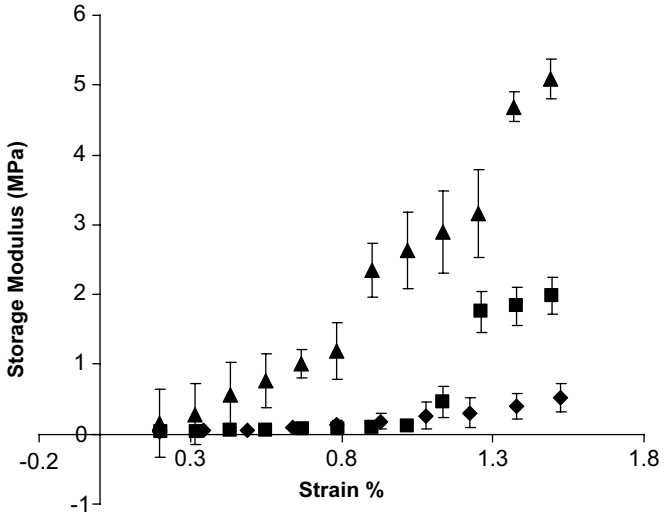

Fig. 5. Storage modulus of 12 wt% SELP hydrogels (cured for 4 h) under multi-strain sweep using dynamic mechanical analysis (DMA). Symbols represent SELP-47K (▲), SELP-415K(◆) and SELP-815K (■). Bars represent standard deviation ($n = 3$).

3.6. Small-angle neutron scattering (SANS)

SANS allows the examination of microstructures in the range 1–100 nm through the analysis of elastic neutron scattering from SELPs [17]. SANS has been successfully used to characterize a wide range of structures in synthetic and natural polymer systems [23,24]. The static structure of solid SELP hydrogels (post-gelation) and the kinetic analysis of sol-to-gel transition at 37 °C were investigated using SANS. SANS analysis was used to examine the correlation between the observed macroscopic properties of SELPs such as equilibrium swelling, mechanical modulus, and bioactive agent release with the underlying network structure. The SANS scattering curves show systematic changes between SELP molecules implying fundamental differences in the underlying microstructure for the SELP-47K, -415K, and -815K samples (Fig. 6A). The data was fit using a combined Debye–Bueche/power-law model which revealed trends in the SELP fibril correlation length that confirm observations about structural effects [25].

SELP hydrogels conformed closely with a modified gel model of the general form $I(Q) = AQ^b + (BQ^2\varepsilon^2)^2 + C$, which uses a power-law fit for the high q scattering combined with the Debye–Bueche model at low to intermediate Q (above $Q = 0.02$ Å^{-1}). This model has been used previously to describe structural inhomogeneities in gels [25]. The detailed equation used for the modeling routine [17] was

$$I(Q) = \left(4\pi K\varepsilon^2 \mathrm{corr}L^2\right)/\left(1 + Q^2\mathrm{corr}L^2\right)^2 + AQ^b + C \qquad (2)$$

where $K = 8\pi 2\lambda^{-4}$.

The combined Debye–Bueche/power-law model provided a nearly complete fit over the full q-range of collected data (Fig. 6B–D). This analysis of SELP-47K, -415K, and -815K revealed scattering profiles that, while similar in form, showed characteristic trend in low q power-law scattering and the Debye–Bueche correlation length ($(4\pi K\varepsilon^2\mathrm{corr}L^2)/(1 + Q^2\mathrm{corr}L^2)^2$) (Table 2).

The calculated correlation length (Table 2), depicts a trend in the observation that is in the order SELP-415K > SELP-815K > SELP-47K. This is consistent with the DMA data (Fig. 6) showing that SELP-47K had the highest storage modulus, and with previous results from TEM, swelling and release studies [10,13,22]. Presence of shorter elastin blocks separating the crystallized silk blocks of the SELP-47K compared with the other analogs (415K and 815K) resulted in a stiffer hydrogel with smaller spacing of the crystalline silk units.

In contrast, SELP-415K had the longest correlation length and the lowest storage modulus. The silk blocks of SELP-415K are separated by elastin blocks twice the length at -47K, and as these cross-linking blocks move further apart, the elastin-like nature of the SELP becomes more pronounced and the storage modulus decreases. SELP-815K presents an interesting case where the silk blocks are doubled in length while also having a long elastin block as in SELP-415K. While the larger silk blocks provide improved cross-linking when combined with a 15-unit elastin block, the

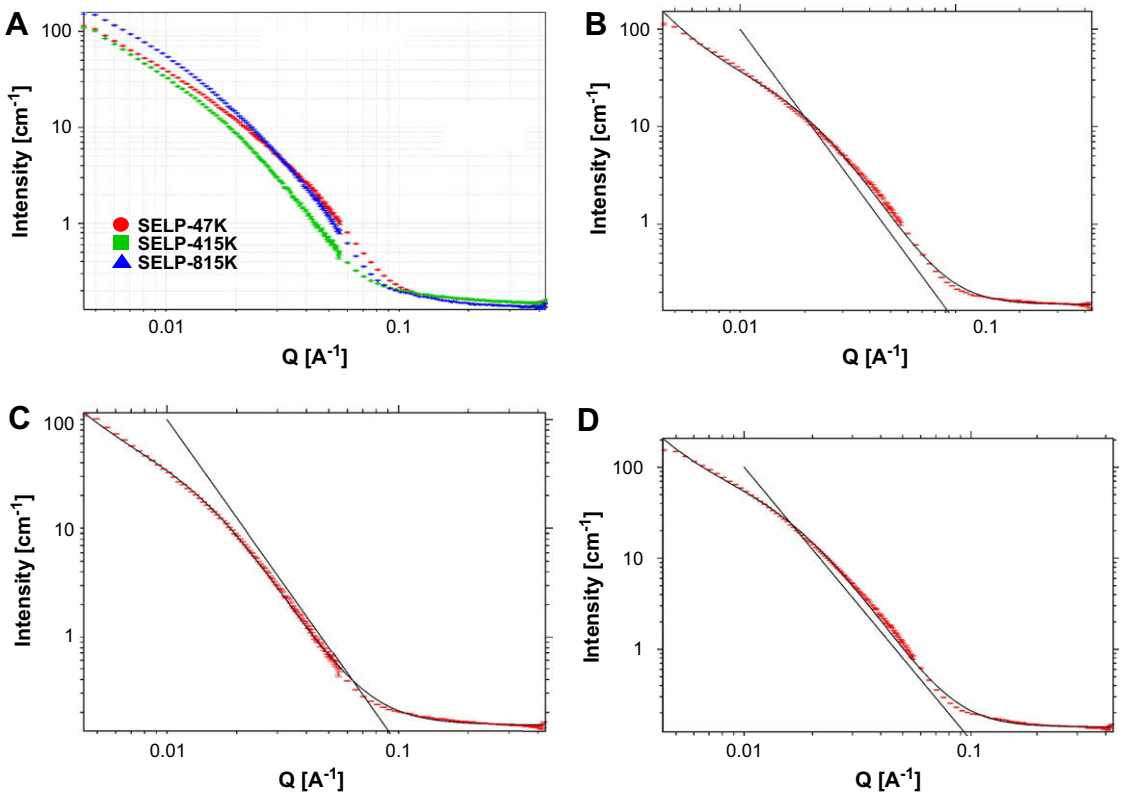

Fig. 6. A. Small-angle neutron scattering plot of 12 wt% SELPs. B–D. Power-law/Debye–Bueche model fit for SANS data from 12 wt% SELPs. B. SELP-47K, C. SELP-415K and D. SELP-815K.

correlation length and storage modulus fall between those of SELP-47K and -415K. The combination of SANS and DMA data together suggests that the elastin block of the SELPs predominantly influences the effective pore size.

Kinetic analysis of the sol-to-gel transition in SELP-47K at 4 wt% and 8 wt% was modeled using the same Debye–Bueche/power-law function. Results reveal a significant drop in correlation length within the first 10 min of gel curing at 37 °C (Fig. 7A) which remains largely constant until the conclusion of the experiment. The calculated power-law slope rises sharply at the same time period as the drop in the correlation length and also then remains approximately constant over the time period studied (Fig. 7B). The drop in correlation length for 10 min occurs within the time frame normally associated with the sol–gel transition of SELPs as observed using rheometry [4]. More interestingly, it was observed that the overall shape of the scattering data over the entire duration of the experiment does not change, significantly, suggesting that the liquid SELP and solid SELP have very similar underlying structures. This suggests a fast initial "nucleation" step with the formation of the cross-links early on, with the aggregation (and crystallization) of silk units leading to the formation of the primary hydrogel structure. In other polymer pre-gel solutions, the scattering profiles are normally dominated by the liquid structure solution, and then

Table 2
Debye–Bueche/power-law model results for SELP hydrogels.

SELP composition (12 wt%)	Power-law low Q slope	Correlation length from Debye–Bueche[a]	Debye–Bueche mid-Q slope
SELP-47K	2.74	4.58 nm ± 0.01 nm	~−3
SELP-415K	2.51	6.55 nm ± 0.78 nm	~−3
SELP-815K	3.26	5.94 nm ± 1.18 nm	~−3

[a] Refer to Equation (2) in the text.

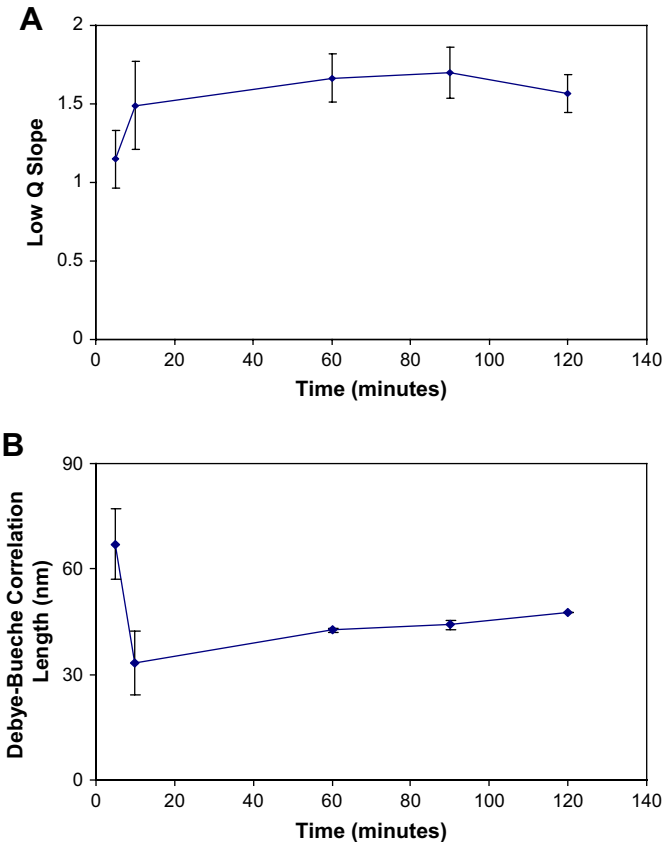

Fig. 7. SANS analysis of the kinetics of sol-to-gel transtion for 4 wt% SELP-47K gelation as a function of time. A. High q slope; B. Debye–Bueche correlation length (nm).

develop significant low q scattering due to frozen inhomogeneities as the cross-linked 3-dimensional structure of the gel forms [23].

The intensity of scattering by SELPs increases with cure time without any significant change in the shape of the scattering curve. This result indicates that although the SELP undergoes a sol–gel transition at 37 °C, the morphology of the fibrillar structure of the SELPs remains largely unaltered. In solution, therefore, the SELPs most likely have a silk block clustering which then evolves to form the cross-linking points retaining the 3-dimensional arrangement as the gel is formed. Given that the calculated correlation length drops from ~68 nm to ~34 nm during the apparent sol–gel transition, it is likely that with increase in cure time additional crosslink points are formed between different SELP fibrils that decrease the average distance between silk-crosslink points. This is consistent with previous results which indicate that with increase in cure time these hydrogels tend to exhibit smaller swelling ratios and release rates, highlighting a slow "consolidation" step where additional cross-links are formed [10,15].

4. Conclusion

A new silk–elastinlike polymer, SELP-815K, was synthesized by recombinant techniques. This polymer has the same silk to elastin ratio as that of SELP-47K, but with similar elastin block length as that of SELP-415K biosynthesized previously [10]. Equilibrium swelling studies indicate that polymer structure and concentration are the predominant factors governing the degree of cross-linking in SELP hydrogels. An increase in gelation time resulted in a higher degree of cross-linking evidenced by lower degree of swelling. An increase in ionic strength of the media resulted in a decrease in the degree of swelling due to counter-ion shielding. Short silk sequences with greater spacing due to longer elastin blocks (as in SELP-415K) rendered the hydrogel sensitive to the changes in temperature. Similar to SELP-815K, SELP-47K was not sensitive to the changes in temperature and pH. Storage moduli (stiffness) of the hydrogels measured by DMA and the correlation length obtained by SANS suggest that the length of the elastin determines the spacing of the cross-links in the hydrogel network while the silk units offer mechanical stiffness and structural rigidity. The polymers were designed to have defined sequences, similar molecular weights and monodispersity. As a consequence the effect of heterogeneity in polymer structure on network properties, as commonly observed with chemically synthesized polymers, was ruled out. These observations suggest that by controlling polymer structure using genetic engineering techniques, SELP hydrogels with controlled and versatile physicochemical and mechanical properties can be developed for a variety of applications including gene delivery and tissue engineering.

Acknowledgement

Funding for this study was provided under NIH R01 CA107621. This work utilized facilities supported in part by the National Science Foundation under Agreement No. DMR-0454672. We acknowledge the support of the National Institute of Standards and Technology, U.S. Department of Commerce, in providing the neutron research facilities used in this work. We would also like to acknowledge the assistance of Wonjoo Lee, Sang Hak Shin, and Mark Laver of NIST in collecting SANS data.

References

[1] Langer R, Tirrell DA. Nature 2004;428(6982):487–92.
[2] Cappello J, Crissman J, Dorman M, Mikolajczak M,, Textor G, Marquet M, et al. Biotechnol Prog 1990;6(3):198–202.
[3] McGrath KP, Tirrell DA, Kawai M, Mason TL, Fournier MJ. Biotechnol Prog 1990;6(3):188–92.
[4] McPherson DT, Morrow C, Minehan DS, Wu J, Hunter E, Urry DW. Biotechnol Prog 1992;8(4):347–52.
[5] Petka WA, Harden JL, McGrath KP, Wirtz D, Tirrell DA. Science 1998;281:389–92.
[6] Meyer DE, Chilkoti A. Nat Biotechnol 1999;17(11):1112–5.
[7] Betre H, Liu W, Zalutsky MR, Chilkoti A, Kraus VB, Setton LA. J Controlled Release 2006;115:175–82.
[8] Nagarsekar A, Crissman J, Crissman M, Ferrari F, Cappello J, Ghandehari H. Biomacromolecules 2003;4(3):602–7.
[9] Cappello J, Crissman JW, Crissman M, Ferrari FA, Textor G, Wallis O, et al. J Controlled Release 1998;53(1–3):105–17.
[10] Haider M, Leung V, Ferrari F, Crissman J, Powell J, Cappello J, et al. Mol Pharm 2005;2(2):139–50.
[11] Megeed Z, Haider M, Li D, O'Malley Jr BW, Cappello J, Ghandehari H. J Controlled Release 2004;94(2–3):433–45.
[12] Hatefi A, Cappello J, Ghandehari H. Pharm Res 2007;24(4):773–9.
[13] Dandu R, Cappello J, Ghandehari H. J Bioact Compat Polym 2008;23:5–19.
[14] Haider M, Cappello J, Ghandehari H, Leong KW. Pharm Res 2008;25(3):692–9.
[15] Dinerman AA, Cappello J, Ghandehari H, Hoag SW. Biomaterials 2002;23(21):4203–10.
[16] Glinka CJ, Barker JG, Hammouda B, Krueger S, Moyert JJ, Orts WJ. J Appl Crystallogr 1998;31(3):430–45.
[17] Ilavsky J. Irena SAS modeling macros manual; January 2008.
[18] Hoffman AS. Adv Drug Delivery Rev 2002;54(1):3–12.
[19] Manno M, Emanuele A, Martorana V, San Biagio PL, Bulone D, Palma-Vittorelli MB, et al. Biopolymers 2001;59(1):51–64.
[20] Dreher MR, Simnick AJ, Fischer K, Smith RJ, Patel A, Schmidt M, et al. J Am Chem Soc 2008;130(2):687–94.
[21] Urry DW. In: Park K, editor. Transductional protein-based polymers as new controlled release vehicles. Washington, DC: American Chemical Society; 1997. p. 405–38.
[22] Cresce AV, Dandu R, Burger A, Cappello J, Ghandehari H. Mol Pharm 2008;5(5):891–7.
[23] Pochan DJ, Pakstis L, Ozbas B, Nowack AP, Deming TJ. Macromolecules 2002;35:5358–60.
[24] Nitash PB. In: Higgins J, Benoit H, editors. Polymers and neutron scattering, vol. 34. Oxford, UK: Clarendon Press; 1996. p. 1827–8.
[25] Debye P, Bueche AM. J Appl Phys 1949;20:518–25.